Supercritical antisolvent coprecipitation mechanisms

Valentina Prosapio, Iolanda De Marco*, Ernesto Reverchon

Department of Industrial Engineering, University of Salerno,

Via Giovanni Paolo II, 132, 84084, Fisciano (SA), ITALY

www.supercriticalfluidgroup.unisa.it

*idemarco@unisa.it Fax: +39-89-964057

ABSTRACT

Supercritical antisolvent precipitation (SAS) has been successfully used to produce microparticles and nanoparticles of controlled size and distribution either as a single precipitates or by coprecipitation of two or more compounds. SAS coprecipitation process has produced different particles morphologies and, differently from the single compound SAS precipitation, process mechanisms involved have never been elucidated and the effectiveness of the technique has been verified only in some cases.

In this work, the mechanisms proposed in SAS coprecipitation are critically discussed and general indications about coprecipitation efficiency are given, based on several experimental evidences and on the possible underlying nucleation, growth and drying mechanisms.

The most effective and reliable SAS coprecipitation resulted from the formation of microdroplets and their subsequent drying.

KEYWORDS: Supercritical Antisolvent, Coprecipitation, Precipitation mechanisms, Microparticles, Nanoparticles.

1. INTRODUCTION

The application of microparticles (MP) and nanoparticles (NP) is relevant in several industrial fields. Microparticles are largely employed in: pharmaceutical industry for aerosol and injectable formulations [1-3]; food industry as emulsifiers, thickener, gelling and stabilizing agents [4-6]; chromatography as stationary phases [7-9]; catalysis as supports [10-12]; coloring industry for the production of inks, toners and paints with improved duration and brightness [13-16]. Nanoparticles promise many applications since at nanoscale matter properties can change considerably: explosives can achieve higher potential, i.e., they approach the ideal detonation [17]; pigments can show more shining colors [18]; polymers can have enhanced functional and structural properties [19, 20]; drugs can exhibit improved bioavailability or can overcome human body internal barriers [21, 22].

Several micronization techniques have been proposed in literature: spray-drying [23, 24], jet milling [25, 26], liquid antisolvent precipitation [27, 28], solvent evaporation [29, 30], emulsification [31, 32] and lyophilization [33]. However, these methods suffer of many drawbacks, mainly lack of control over particle morphology, particle size and particle size distribution (PSD), difficulty in the elimination of the solvents used and possible degradation due to high temperatures employed [34].

An alternative to conventional processes is represented by supercritical carbon dioxide (sc-CO_2) based techniques. Several processes have been proposed to produce micro or nanoparticles: Rapid Expansion of Supercritical Solutions (RESS) [35, 36], Particles from Gas Saturated Solution (PGSS) [37], Supercritical Assisted Atomization (SAA) [38, 39], Supercritical Emulsion Extraction (SEE) [40, 41] and Supercritical Antisolvent (SAS) [42, 43], proposed in the literature also using different acronyms such as Aerosol Solvent Extraction System (ASES) [44], Solution Enhanced Dispersion by Supercritical fluids (SEDS) [45], Supercritical AntiSolvent with Enhanced Mass transfer (SAS-EM) [46]. Among them, SAS is largely the most successful in the processing of pharmaceuticals, coloring

matters, explosive, polymers and biopolymers [47-51] with a good control over particle size and particle size distribution (PSD); SAS process allows the production of micro or nanoparticles, depending on the specific process conditions selected [52]. It is based on two prerequisites: the solvent and the antisolvent (CO_2) must be completely miscible at process conditions; the solute must be insoluble in the mixture solvent/antisolvent. Different precipitates' morphologies have been obtained by SAS: nanoparticles with a mean size in the range 30-200 nm [53, 54], microparticles in the range 0.25-20 μm [47, 55], expanded hollow microparticles (also called balloons) with diameters between about 10 and 200 μm [56, 57] and crystals with micrometric dimensions and various habits [58, 59]. The main limitation of SAS is the difficulty to process some categories of materials: (i) molecules soluble in CO_2 and/or in the mixture solvent/antisolvent; (ii) water-soluble compounds, because of the wide miscibility gap between water and CO_2 at the ordinary SAS operating conditions (40-60 °C, 100-250 bar) [60]. The latter limitation has been recently overcome using a SAS modification, named Expanded Liquid Antisolvent (ELAS) [61] that employs a mixture of CO_2 and an organic polar solvent at expanded liquid conditions to improve water solubility in the gaseous mixture; ELAS was successfully applied to the micronization of proteins, enzymes and polymers [6, 62].

However, in many applications, the coprecipitation of two or more compounds is required. For example, labile molecules, such as vitamins and antioxidants, require generally encapsulation to protect them from degradation [63], drugs can be incorporated into polymeric matrices to control and/or enhance their release kinetics [64] and food ingredients may require a carrier to mask their taste or odor [65]. These composite particles can be produced in form of microspheres or microcapsules. In the former, the polymer and the drug are uniformly dispersed within the same particle; whereas, in the latter a polymeric shell surrounds the drug. In both cases, it is possible to assert that the two solutes are coprecipitated.

71 Despite SAS coprecipitation has been studied by several authors, general rules have not been
72 proposed so far and the precipitation mechanisms have not been elucidated. The aim of the present
73 work is therefore to discuss the mechanisms involved in SAS coprecipitation and to propose general
74 indications for successful coprecipitation.

75 ## 2. METHODS

76 *2.1 SAS apparatus*

77 A generic sketch of SAS apparatus is reported in Figure 1. It is equipped with two pumps used to
78 feed the liquid solution and supercritical CO_2, respectively. A cylindrical vessel is used as the
79 precipitation chamber. The liquid solution is delivered to the precipitator through a thin wall
80 stainless steel nozzle. The temperature control is assured by a controller connected with electrically
81 thin bands and the pressure in the vessel is measured using a manometer and regulated by a
82 micrometering valve. The collection of the produced powders occurs using a stainless steel filter,
83 located at the bottom of the precipitator that also allows the CO_2-organic solvent solution to pass
84 through. A second collection vessel, located downstream the micrometering valve, is used to
85 recover the liquid solvent.

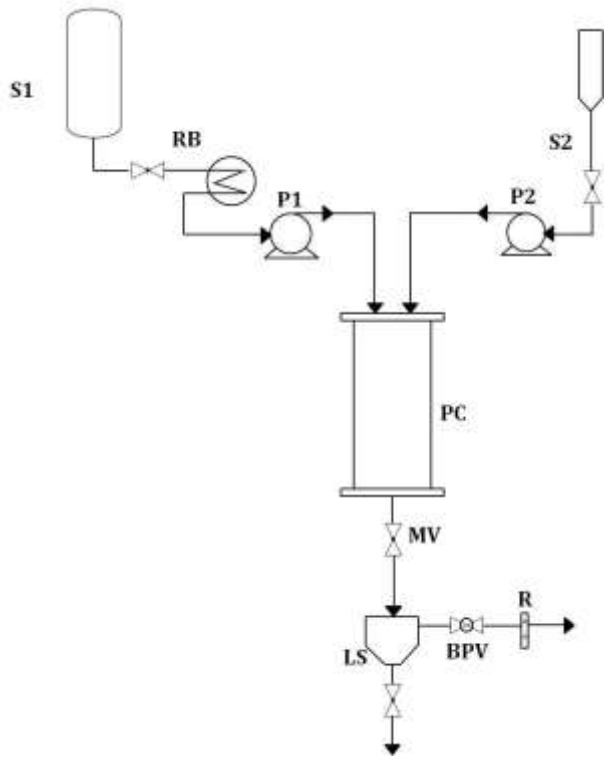

Figure 1: Schematic representation of SAS apparatus. S1: CO_2 supply; S2: liquid solution supply; RB: refrigerating bath; P1, P2: pumps; PC: precipitation chamber; MV: micrometering valve; LS: liquid separator; BPV: back-pressure valve; R: rotameter.

Common modifications of SAS involve the use of different kinds of nozzle:

- capillary nozzle with ultrasonic vibrating surface (SAS-EM, Supercritical Antisolvent with Enhanced Mass transfer), which can produce smaller and more uniform particles [46, 66, 67];
- coaxial nozzle (SEDS, Solution-Enhanced Dispersion by supercritical fluids, and ASES, Aerosol Solvent Extraction System) in which carbon dioxide and the feed solution are delivered through the same orifice: in this way, sc-CO_2 is employed not only as antisolvent but also as spray enhancer [48, 68];
- jet-swirl nozzle, to enhance mixing of the fluids, producing a gaseous swirling hollow-core annular jet [69, 70].

2.2 SAS procedure

A SAS experiment starts delivering CO_2 at a constant flow rate to the precipitation chamber until the desired pressure is reached. Then, pure solvent is sent through the nozzle in the precipitator to obtain steady state composition conditions of the fluid phase during the solute precipitation. When a quasi-steady state composition of solvents and antisolvent is realized inside the vessel, the flow of the solvents is stopped and the liquid solution, at the given flow rate, is fed through the injector, causing the precipitation of the solute. When the solution delivery is completed, only supercritical CO_2 is flushed, with the aim to remove the solution formed by the liquid solubilized in the supercritical antisolvent. Finally, CO_2 flow is stopped, the precipitator is gradually depressurized down to atmospheric pressure and it is possible to recover the dry powders from the porous filter.

3. RESULTS AND DISCUSSION

The analysis of scientific literature showed that more than one hundred papers on SAS coprecipitation have been published on relevant international journals, mainly between 2010 and 2017, using about 20 different polymers as coprecipitating agents, the most successful being PLLA and PVP. Active principles that the authors tried to coprecipitate cover several areas; mainly pharmaceutical and nutraceutical.

In Table 1, a selected list of SAS coprecipitates is reported; it contains indication about operating conditions employed, obtained morphologies as described by the authors and particle mean size when measured. The carbon dioxide molar fraction chosen for the successful SAS processing is generally in the range 0.95-0.99.

Table 1: Overview of SAS coprecipitation results proposed in the literature.

Polymer	API	Solvent	P, bar	T, °C	C_{TOT}, mg/mL	Morphology	D, µm	Ref, authors, year
β-CD	Lycopene	DMF	100-140	40-50	1.1	NP	0.04-0.12	[71], Nerome et al., 2013
CAP	Quercetin	AC	90	40	20.0	NP + C	-	[72], García-Casas et al, 2017
EC	Amoxicillin	DMSO/DCM	100-250	35-65	10.0	Coalescing MP	0.23-2.66	[64], Montes et al., 2011
	Ampicillin	DMSO/DCM	100-250	35-55	11.3	Coalescing MP	1.0-3.0	[73], Montes et al., 2012
	Rifampicin	EtAc	100	35-60	12.5-15.0	NP+C	-	[74], Djerafi et al., 2017
		EtAc/DMSO				NP	0.19-0.23	
Eudragit	Ellagic acid	NMP	150	40	20.0	MP+C	-	[75], Montes et al., 2016
	Ibuprofen	AC	120-200	40	5.0-10.0	NP	0.08-0.21	[76], Montes et al., 2014
			120	50	5.0	SMP	0.51	
	Magnetite	EtOH	160	15-35	5.0-10.0	NP	< 0.2	[77], Lam et al., 2012
	Naproxen	EtOH	150-200	40-50	5.0-8.0	NP	0.08-0.15	[78], Montes et al., 2014
			100	40	5	SMP	0.31	
HPC	Ezetimibe	EtOH	120-180	40-50	10.0-25.0	NP	0.15-0.24	[79], Ha et al., 2015
			150	40	50.0-100.0	SMP-MP	0.33-0.91	
HPMC	Insulin	DMSO/AC	120	32	2.0	NP	0.14	[80], Jin et al., 2012
					3.7-7.0	SMP	0.27-0.34	

	Lercanidipine	EtOH/DCM	150	40	50.0	NP-SMP	0.22-0.40	[81], Ha et al., 2015
	Megestrol acetate	EtOH/DCM	150	40	52.0	NP-SMP	0.14-0.50	[82], Ha et al., 2015
	Telmisartan	EtOH/DCM	120	45	25.0	SMP	0.45-0.50	[83], Park et al., 2013
Lactose	Rifampicin	MeOH	124	40	1.0-5.0	Coalescing MP	< 8.0	[84], Ober et al., 2013
Lecithin/α-tocopherol	Lycopene	DMF	80-120	35	20.0-30.0	C	-	[85], Cheng et al., 2017
PCL	Green tea	AC	80-120	10-34	Not rep.	Coalescing MP	3.0-5.0	[86], Sosa et al., 2013
PEG	β-carotene	DCM	80	35	13.2-17.2	MP+C	-	[87], Martín et al., 2007
	Carotene	DCM	160	35-50	6.0	MP+C	1.0-10.0	[88], He et al., 2007
	Emodin	DCM/MeOH	80-200	35-50	1.0	C	3.0-20.0	[89], Lang et al., 2012
	Itraconazole	AC	190	40	2.0	MP+C	3.0	[90], Barrett et al., 2007
	Lutein	DCM	80-100	15	13.2-15.0	Coalescing MP	5.0-50.0	[87], Martín et al., 2007
	Oxeglitazar	CHF	80	35	30.0	C	-	[91], Majerik et al., 2007
mPEG-PLLA	Leuprolide acetate	DCM/MeOH	130	35	10.5-12.0	MP	2.86-5.63	[92], Jung et al., 2012
PHBV	β-carotene	DCM	80	40	32.3-60.8	C	-	[93-95], Franceschi et al., 2008; 2010; Priamo et al., 2010
	Astaxanthin	DCM	80-100	35	5.0-10.0	SMP	0.22-0.40	[96], Machado et al., 2016
	Bixin	DCM	80-100	35-40	1.4-20.4	SMP	0.20-0.55	[45], Boschetto et al., 2014
	Grape seed extract	DCM	80-120	35-45	26.7-40.0	SMP	0.62-0.72	[97], Boschetto et al., 2013
PLA	Azacytidine	DMSO/DCM	110	40	19.0	MP+C	2.0	[98], Argemì et al., 2009

	Budesonide	DCM	85.8	40	14.0	MP	1.26	[99], Martin et al., 2002
	Cholesterol	DCM	90	45	9.8	MP	1.70	[100], Guha et al., 2011
					46.3	C	8.0	
	Ibuprofen	DCM	120-200	40-50	5.0-10.0	MP	0.93-1.97	[76], Montes et al., 2014
	Insulin	DMSO/DCM	85-130	20-38	1.0	MP	0.50-2.0	[101], Elvassore et al., 2001
	Lutein	EtAc	100	17	21.8-22.2	Coalescing MP	1.0-10.0	[102], Miguel et al., 2008
	Naproxen	DCM	100-200	40-50	5.0-8.0	MP	0.56-1.43	[78], Montes et al., 2014
PLA/PCL	17α-methyltestosterone	DCM	80	40	0.01	MP	23.0-54.0	[103], Sacchetin et al., 2016
PLGA	5-Fluoracil	AC	110	36	6.0	Film	-	[104], Kalantarian et al., 2011
		DCM/MeOH	110	36	6	Coalescing MP	-	
			110	36-45	6.0-30.0	Film	-	
	Bupivacaine HCl	EtOH/DCM	80	40	Not rep.	MP+Fibers	5.56-7.07	[105], Lee et al., 2006
	Hydrocortisone	AC	89.6	33	20.0	C	-	[106], Wang et al., 2006
		MeOH/DCM	89.6	33	20.0	C	-	
	Passion fruit seed oil	DCM	90	35-45	32.0	MP	0.83-1.50	[107], Oliveira et al., 2017
			110	35-45	32.0	Coalescing MP	-	
	Silica	AC	89.6-110	33-42.5	Not rep.	MP	0.55-24.8	[67], Wang et al., 2005
PLGA/PLLA	Bupivacaine HCl	EtOH/DCM	80	40	Not rep.	MP	4.71-10.9	[105], Lee et al., 2006
PLLA	5-Fluoracil	EtOH/DCM	120	33	4.0	MP	0.98	[108], Chen et al., 2006

	10-hydroxycamptothecin	EtOH/DCM	75-120	30-40	1.0-9.0	MP	0.57-1.37	[34], Wang et al., 2013
	Amoxicillin	DMSO/DCM	100-200	29-50	2.0-9.0	MP	Not rep.	[109], Kalogiannis et al., 2006
	Azacytidine	DMSO/DCM	110	40	19.0	MP+C	2.0	[98], Argemì et al., 2009
	Bupivacaine HCl	EtOH/DCM	80	40	Not rep.	MP	4.39-5.53	[105], Lee et al., 2006
	Diuron	DCM	100	35	36.0	MP+C	Not rep.	[110], Taki et al., 2001
			100	35	14.0-25.0	MP	Not rep.	
	Leuprolide acetate	DCM/MeOH	130	35	10.5-12.0	MP	Not rep	[92], Jung et al., 2012
	Paclitaxel	DCM	120	35	7.0	MP	0.83	[111, 112], Li et al., 2012; Wenfeng et al., 2012
		DCM/DMSO	120	35	7.0	MP	0.84-0.89	
		DCM/EtOH	80-140	30-45	7.0-14.0	MP	0.91-1.43	
	Rifampicin	DCM	138-207	33-50	10.0-30.0	MP	3.26-30.53	[113], Patomchaiviwat et al., 2008
	Tamoxifen citrate	DCM	130	38	13.5	MP	Not rep	[114], Alias et al., 2017
	Zidovudine	EtOH/DCM	85-135	45	0.2	Filaments	-	[115], Yoshida et al., 2015
Pluronic	Astaxanthin	AC	80-120	35-40	6.0	Coalescing MP	-	[116], Mezzomo et al., 2012
	Quercetin	AC	100	40	0.03-0.2	Coalescing MP	1.00	[117], Fraile et al., 2014
Poloxamer	Oxeglitazar	EtOH/CHF	80	35	23.0	C	-	[91], Majerik et al., 2007
		DCM	80	35	27.0	C	-	
PVM/MA	Gentamicin-AOT	AC	100	25	140.0	NP-MP	0.05-0.93	[118], Elizondo et al., 2011
PVP	α-tocopherol	DMSO	90-150	35-50	20.0-60.0	MP	1.80-4.08	[119], Prosapio et al., 2017

	β-carotene	AC/EtOH	85-100	40	5.0-7.0	MP	0.80-2.43	[120], Prosapio et al., 2015
	β-carotene*	AC/EtOH	85	40	5.0	NP	0.25	
	Budesonide	EtOH	90	40	20.0	MP	3.06-3.58	[121], Prosapio et al., 2016
	Curcumin	AC/EtOH	100-200	30-50	1.0-10.0	NP-SMP	0.03-0.34	[70], Chhouk et al., 2017
	Dexamethasone	EtOH	90	40	20.0	MP	1.82-2.51	[121], Prosapio et al., 2016
	Diflunisal	AC/DCM	120-140	35	18.0-36.0	Coalescing MP	2.80-8.10	[122], Zahran et al., 2014
	Ezetimibe	EtOH	150	40	25.0	NP	0.21-0.23	[79], Ha et al., 2015
	Folic acid	DMSO	90-130	35-40	20.0-40.0	MP	0.30-3.80	[123], Prosapio et al., 2015
			150	40	40.0	NP	0.05-0.20	
	Hydrochlorothiazide	DMSO	86-190	30-40	10.0-30.0	NP	0.15-0.21	[124], Park et al., 2017
		DMSO/AC	135	30	10.0	NP	0.05-0.09	
	Menadione	DMSO	90-150	35-50	20.0-60.0	MP	2.64-5.09	[119], Prosapio et al., 2017
	Nimesulide	DMSO	90-150	35-45	20.0-35.0	MP	1.67-4.04	[125], Prosapio et al., 2016
	Oxeglitazar	EtOH/CHF	80	35	30.0	C	Not rep	[91], Majerik et al., 2007
	Piroxicam	DCM	96.5	25	0.05	MP	Not rep.	[126], Wu et al., 2009
	Prednisolone	EtOH	90-150	40	10.0-30.0	MP	1.96-3.03	[121], Prosapio et al., 2016
	Telmisartan	EtOH/DCM	120	45	25.0	MP	0.38-0.60	[83], Park et al., 2013
Zein	Lutein	AC/DMSO	100	32-45	10.0-20.0	SMP	0.20-0.36	[127], Hu et al., 2012

API: active pharmaceutical ingredient; D: mean diameter; NP: nanoparticles; MP; microparticles; SMP: sub-microparticles; C: crystal. Not rep.: information not reported.

AC: acetone; CHF: chloroform; EtAc: Ethyl acetate; EtOH: ethanol; DCM: dichloromethane; DMF: dimethylformamide; DMSO: dimethylsulfoxide; MeOH: methanol; NMP: N-methyl-2-pyrrolidone.

β-CD: β-cyclodextrin; CAP: cellulose acetate phthalate; EC: ethyl cellulose; HP-β-CD: hydroxypropyl-β-cyclodextrin; HPC: hydroxypropyl cellulose; HPMC: hydroxypropylmethyl cellulose; PCL: poly(ε-caprolactone); PEG: poly-ethylene glycol; mPEG-PLLA: methoxy poly(ethylene glycol)-b-poly(L-lactide); PHBV: poly(hydroxybutirate-co-hydroxyvalerate); PLA: polylactic acid; PLGA: poly(lactide-co-glycolide); PLLA: poly(L-lactic acid); PVA: polyvinyl alcohol; PVM/MA: polymer poly (methyl vinyl ether-co-maleic anhydride); PVP: poly(vinylpyrrolidone). *Use of PVP with 40 kg/mol molecular weight

As reported in Table 1, depending on the employed materials and on the operating conditions, different morphologies have been observed for SAS coprecipitation: irregular and/or coalescing particles; microparticles; nanoparticles; sub-microparticles; crystals; coexistence of crystals, films and particles.

A reference point about the possible morphologies that can be obtained by SAS coprecipitation can be given by morphologies already observed in the case of SAS precipitation of single compounds and the explanation given for them in the literature. Nanoparticles are generally observed when SAS is performed at completely developed supercritical conditions, i.e. at pressure values far above the mixture critical point (MCP) of the binary mixture solvent/antisolvent. Operating at these conditions, the jet break-up time (t_1) is longer than the interfacial tension vanishing time (t_2) and nanoparticles are obtained by a gas-to-particle nucleation and growth mechanism [52, 128-132]. Microparticles are usually observed when the operating point is located near above the MCP [133]. In this case, t_2 is longer than t_1 and microparticles are formed as a result of the liquid jet atomization and the very fast solvent extraction operated by sc-CO_2 [52]. Crystals with different shape and size can be produced when the operating point falls within the two-phase region of the vapor liquid equilibria (VLE) diagram; in this case, a liquid-like crystallization mechanism takes place, in which nuclei are formed in the liquid-phase and grow is due to the continuous migration of molecules from the liquid towards the surface of the forming crystal [52]. Furthermore, the hydrodynamics' conditions are also important and have to be controlled in SAS coprecipitation, since flow and mixing conditions have a significant influence upon mass transfer kinetics and thus on the characteristics of the formed particles [128, 134].

3.1 Coprecipitation results

3.1.1 Microparticles

Jung at al. [92] proposed the encapsulation of Leuprolide acetate with mPEG-PLLA and PLLA using a mixture of DCM/MeOH as solvent and 130 bar, 35 °C as operating conditions. They observed that the nature of the carrier has a great influence on the precipitate morphology. Specifically, spherical MP with a smooth surface and an entrapment efficiency (EE %) equal to 99 % were produced when PLLA molecular weight (Mw) was higher than 12000 Da; whereas, an irregular and coalescing material with moderate EE was obtained in correspondence of lower Mw. Moreover, they observed that particle mean size became larger increasing the PEG block length. The authors found that drug release was faster when mPEG-PLLA was employed as carrier and the rate was higher increasing the content of PEG in the formulation; however, they did not report the dissolution profile of the pure drug as a comparison, to show the benefit provided by coprecipitation. Prosapio et al. [120] also investigated the effect of polymer molecular weight in the production of PVP/β-carotene from AC/EtOH; they found that MP were obtained at a pressure of 85-100 bar, a temperature of 40 °C, a carbon dioxide molar fraction equal to 0.98, and a concentration of the liquid solution in the range 5.0-7.0 mg/mL using a 10 kg/mol PVP, whereas increasing Mw at 40 kg/mol the precipitation of NP was observed. In vitro drug release tests showed that, for SAS processed composite microparticles, the dissolution rate of the vitamin was 10 times faster than for unprocessed β-carotene. Park et al. [83] studied the coprecipitation of Telmisartan with HMPC and PVP using DCM as solvent, at 120 bar and 45 °C. They observed that, at the same process conditions, coalescing sub-microparticles (SMP) were produced employing HPMC; whereas, well separated spherical SMP were obtained using PVP. For all samples, in vitro dissolution tests were carried out; it was observed that the drug dissolution rate was largely improved for SAS polymer/drug particles, but it was comparable with the dissolution rate of SAS processed Telmisartan (without the polymer). Lee et al. [105] used PLGA, PLLA and PLGA/PLLA for the coprecipitation of Bupivacaine HCl from EtOH/DCM at 80 bar and 40 °C. They observed that, when PLGA was used as carrier, irregular and

rough MP together with fibers were obtained and hypothesized that those filaments were formed by the drug, whereas the particles were formed by the polymer; when PLLA and PLGA/PLLA were used, MP were obtained. Drug release tests were performed to verify the ability of SAS processed particles to allow a sustained release of the water-soluble drug. They showed that particles produced using PLGA released the drug in 30 min, confirming that for those samples coprecipitation failed; particles obtained using PLLA and PLGA/PLLA showed a very significant decrease in the drug dissolution rate (release was longer than 7 days), demonstrating the occurrence of the coprecipitation. Reverchon and coworkers proposed in some papers a systematic investigation of the effect of the polymer/drug ratio. They coprecipitated PVP with Folic acid [123], β-carotene [120], Corticosteroids [121], Nimesulide [125] and some liposoluble vitamins [119]. Two examples of microparticles produced using different active principles, different organic solvent and different operating conditions are shown in Figure 2, where unpublished FESEM images of PVP/Prednisolone and PVP/Menadione are reported that clearly indicate the morphology observed.

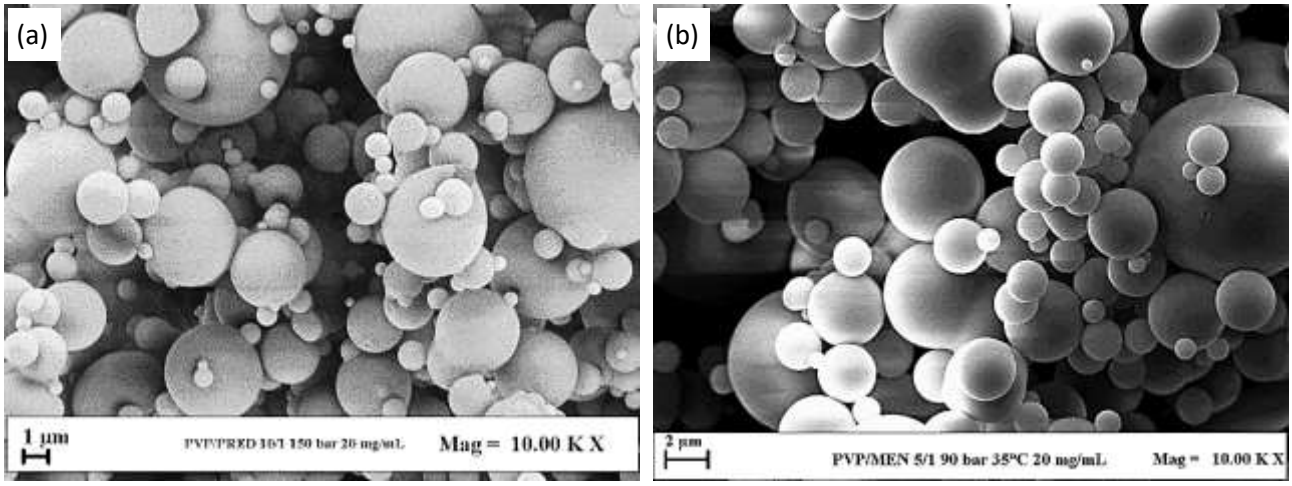

Figure 2: FESEM images of microparticles; (a) PVP/Prednisolone precipitated from Ethanol at 150 bar, 40 °C and 20 mg/mL (unpublished image related to [121]); (b) PVP/Menadione precipitated from DMSO at 90 bar, 35 °C and 20 mg/mL (unpublished image related to [119]).

They observed that at low ratios, i.e. 1/1 and 2/1 w/w, generally compounds precipitated in form of coalescing material and crystals; this evidence suggests that they precipitated separately.

On the other hand, rising the polymer/drug ratio from 3/1 to 10/1 w/w, spherical microparticles were produced and it was consistently observed that increasing the amount of PVP, particle mean size increased and PSD enlarged. In addition, the authors demonstrated that the active pharmaceutical ingredient (API) dissolution rate was largely enhanced only in the case of microsphere production, since in the case of nanoparticles the drug dissolution profile was similar to the SAS processed drug. In their papers, they also highlighted the role of PVP in retarding the crystal growth of the drug, thus allowing the formation of spherical MP. Analogous results were referred by Li et al. [126] in the coprecipitation of PVP/Piroxicam. Zahran et al. [122] also employed PVP for the encapsulation of Diflunisal working at 35 °C and 120-140 bar. They obtained coalescing MP, but particle aggregation reduced increasing the polymer/drug ratio. Drug release tests showed a substantial improvement of the drug dissolution rate compared to pure Diflunisal. Similar evidences were observed by Patomchaiviwat et al. [135] and Hu et al. [127] in the coprecipitation of PLLA/Rifampicin and Zein/Lutein, respectively: MP were obtained using a high polymer/drug ratio; whereas, agglomerated MP were obtained increasing the amount of drug. Fraile et al. [117] studied the coprecipitation of Pluronic and Quercetin from AC at 100 bar and 40 °C; they observed that for polymer/active principle ratios in the range 1/1 to 1.7/1 w/w irregular and slightly coalescing MP with improved dissolution rate were obtained; whereas, using ratios 2/1 and 9/1 w/w, plastification occurred. Guha et al. [100] studied the coprecipitation of PLA and Cholesterol from DCM at 90 bar and 45 °C; they observed that for a polymer/active principle ratio equal to 0.5/1, encapsulated spherical particles were formed, whereas, for a ratio equal to 5/1 long needle-shaped particles were obtained. The authors tried to model the coprecipitation process. They proposed a sort of “single droplet – multiple particles” formation process; but, there are no experimental evidences of this kind of mechanism, which seems to make sense only when multiple nucleation points form in the droplet; in this case, only crystalline particles, and not amorphous ones, have to

be produced. Montes et al. proposed polymer/drug coprecipitation for Ibuprofene [76] and Naproxen [78] using PLA and DMC at 100-200 bar and 40-50 °C. In both papers, the authors reported that the dissolution rate of the unprocessed drug was faster than the SAS processed particles; to explain this result, they hypothesized that probably part of the drug was not dispersed in the polymeric matrix but remained on its surface. They investigated the influence of the polymer/drug ratio in the processing of Eudragit/Ellanic acid [136] from NMP at 150 bar and 40 °C; in all the experiments the presence of coalescing MP and crystals was observed but, increasing the ratio from 1/1 to 4/1, the amount of crystals reduced. The authors also proposed the coprecipitation of Amoxicillin [64] and Ampicillin [73] using EC as carrier for prolonged release applications. Using DCM/DMSO at 100-250 bar and 35-65 °C, they obtained coalescing MP; in vitro release tests in simulates gastric fluid (SGF) and simulated intestinal fluid (SIF) showed that for SAS processed samples the drug release rate was significantly reduced. Chen et al. [108] proposed the coprecipitation of 5-Fluorouracil with PLLA using EtOH/DCM at 120 bar and 33 °C. They stated that spherical microparticles with narrow particles size distribution were produced; however, looking at the SEM image reported in the paper, two populations of particles are clearly visible. This may suggest that coprecipitation failed, leading the formation of a physical mixture of larger particles (likely the polymer, since it precipitated alone in form of large MP) and smaller particles (probably the drug, which precipitated in form of SMP). A comparison between the drug release kinetics of pure drug and SAS processed powder to demonstrate the occurrence of coprecipitation was not performed. Sacchetin et al. [103] proposed the incorporation of 17α-methyltestosterone in PLA/PCL to protect the hormone from degradation in the gastric fluid, thus allowing the release in the intestinal environment. They obtained large MP with incorporation efficiency in the range 20.3-50.5 %. Dissolution tests for SAS processed particles, performed at different pH, did not show a precise trend: the hormone was released slowly at pH 2.2 and 7.4 but was released faster at pH 8.8 and 5.0;

moreover, the dissolution profile of the raw material was not reported as a comparison. Boschetto et al. and Machado et al. used PHBV for the incorporation of Astaxanthin [96], Bixin [45] and Grape seed extract [97] using DCM as solvent and operating at 80-120 bar and 35-45 °C. They obtained SMP at all the operating conditions and observed that, for Astaxanthin and Grape seed extract, encapsulation efficiency was higher increasing the concentration and decreasing the pressure;in both papers, dissolution tests were not performed to demonstrate the success of coprecipitation. In the case of Bixin, a definite trend in the encapsulation efficiency was not found; dissolution tests were performed in different solvents; but, they were not compared with the behavior of pure API. Several authors [84, 86, 87, 102, 116] observed the precipitation of irregular and coalescing particles, but they did not report analyses to verify the success or failure of coprecipitation.

Some papers [67, 99, 101, 120] studied the effect of the concentration of solutes in the liquid solvent on particle morphology; they observed that increasing the concentration, a larger degree of coalescence occurs, with the formation of agglomerates. In particular, Taki et al. [110] observed in processing of PLLA and Diuron, concentrations in the range 14-25 mg/mL led to the precipitation of spherical MP; whereas, increasing this parameter at 36 mg/mL the presence of MP and crystals was noted, suggesting a possible failure of the coprecipitation. Dissolution tests were not performed to investigate further this aspect.

Several works [64, 67, 73, 101, 111, 137] investigated the influence of the operating temperature on SAS coprecipitates and observed that rising this parameter, not only particle size increased, but also evidences of agglomeration were noted; however, indication about the effect of temperature on the success of coprecipitation was not reported. Prosapio et al. [125], in the coprecipitation of PVP with Nimesulide from DMSO at 90 bar and 35-45 °C, obtained well separated spherical MP and observed that, increasing the temperature, particle mean size increased and the PSD broadened. The cumulative particle size distributions are reported in Figure 3 (adapted from [125]).

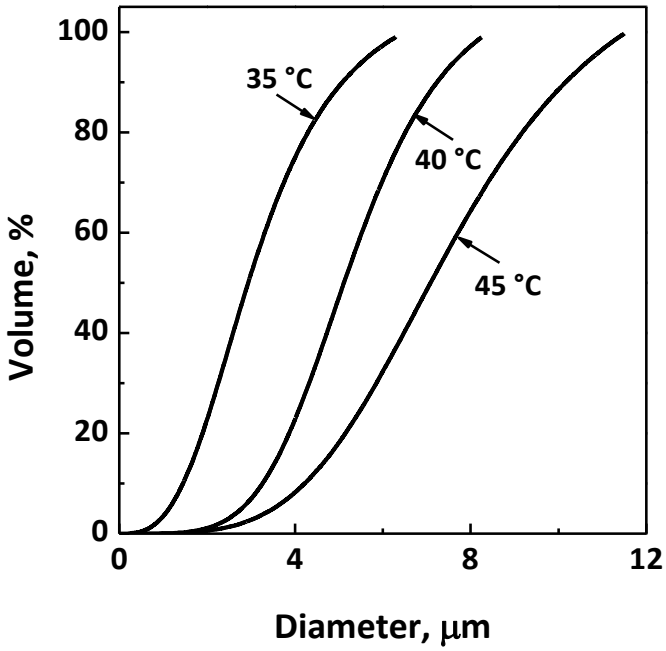

Figure 3: Volumetric cumulative particle size distributions of PVP/Nimesulide microparticles obtained from DMSO at 90 bar, 30 mg/mL at different temperatures (adapted from [125]).

An analogous result was obtained by Montes et al. [76] during processing of Eudragit/Ibuprofen from AC: increasing the temperature from 40 to 50 °C, the powder morphology changed from NP to SMP, with an increase of mean particle size and PSD.

Oliveira et al. [107] proposed the encapsulation of passion fruit seed oil with PLGA from DCM. They obtained MP working at 90 bar and 35-45 °C and coalescing particles when the pressure was fixed at 110 bar; release tests for SAS processed particles were reported, but, they were not compared with the dissolution profile of the pure material to confirm the occurrence of coprecipitation. Wang et al. [137] proposed the coprecipitation of 10-hydroxycamptothecin and PLLA from EtOH/DCM. They observed that, varying the operating pressure from 75 up to 120 bar at 35-40 °C, microparticles were constantly obtained, and the loading increased. In this paper, TEM images showed that particles were characterized by dark areas that the authors referred to the presence of the drug; nevertheless, the release curve of pure 10-hydroxycamptothecin was not reported as a comparison to show if its bioavailability was improved. Prosapio et al. [123] also

investigated the effect of pressure for the system PVP/folic acid using DMSO as solvent. They found that microparticles could be obtained only working at pressures near the MCP of the binary mixture CO_2/DMSO; whereas, nanoparticles were obtained operating far above the MCP. Interestingly, in vitro release analyses showed that only for MP coprecipitation was successful since the vitamin dissolution rate was largely improved: it was 45 times faster than unprocessed folic acid and 23 times faster than SAS processed vitamin, as shown in Figure 4 (adapted from [123]).

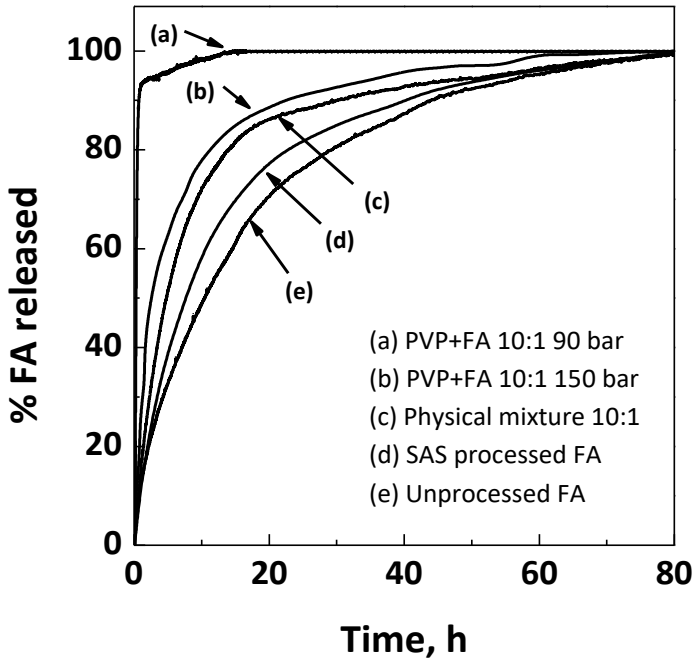

Figure 4: Dissolution profiles of folic acid (adapted from [123]).

Kalogiannis at al. [138] studied the influence of the kind of solvent using mixtures DCM/DMSO at different proportions; they affirmed that, in the range 100-200 bar and 40-50 °C, an increase in DMSO content had a positive effect on the coprecipitation of Amoxicillin in the PLLA matrix. However, the loading efficiency of the produced powder was quite low, 0.9-42.9 %, and dissolution tests or other analyses to confirm the effective formation of composite microparticles were not performed. Different results were found by Li et al. [111] that investigated the use of DCM and the mixtures DCM/DMSO and DCM/EtOH at different ratios in the coprecipitation of Paclitaxel/PLLA. They observed the production of non-spherical MP when DMSO was used as co-solvent and,

increasing its content, higher agglomeration and lower loading were obtained; when ethanol was employed, the presence of fibers was observed, suggesting a failure in the coprecipitation. However, analyses aimed at investigating the composition of the produced particles were not performed.

Comparing the experimental evidences reported in SAS literature for microparticles obtained by coprecipitation, it is possible to identify some key points for the success of coprecipitation. The proper selection of the carrier plays an important role since the polymer ability to influence the precipitation mechanism of the drug can induce the formation of composite microparticles. From the literature review, one can state that the most suitable polymers for coprecipitation are PVP and PLLA, since they generally allow the production of well separate spherical MP with good drug entrapment efficiency. It is also interesting to highlight that often compounds that precipitate in a specific morphology when processed by SAS as single compounds do not show the same behavior when processed in conjunction with another compound.

In order to explain the aforementioned experimental evidences, it is possible to recall the jet break-up mechanisms and droplets formation discussed in the first part of section 3; jet break-up is favoured at near critical conditions [52]. It is reasonable that, when two compounds are dissolved in the liquid solution, droplets formed during jet break-up are formed by both materials arranged in a disordered manner and, upon drying by sc-CO_2, they form composite microparticles in which the two compounds are contained. The prevailing compound (as a rule the polymer) will form a matrix in which the other solute is dispersed in form of nanoparticles. Until now direct evidences of the formation of co-solute nanoparticles inside the polymer matrix have not been proposed; however, the large modification of the drug release observed confirmed this hypothesis.

In many papers, it has been observed the production of coalescing MP. This effect could be caused by several reasons:

- High residual solvent, which occurs when downstream the injection process, the vessel is not flushed with CO_2 for sufficient time to completely remove the solvent solubilized in the supercritical antisolvent;
- Use of high concentrations that makes the feed solution highly viscous and at this condition atomization may fail;
- Use of high temperatures that can cause degradation of the compounds.

Summarizing these results, the production of SAS coprecipitates in form of microparticles is generally an indication of successful processing of the system polymer-drug studied. SAS processing conditions and the precipitation mechanism are similar to those previously proposed for the SAS precipitation of a single compound.

However, there is not guarantee that SAS coprecipitation of two compounds (polymer – active compound) that were previously, singularly, successful SAS precipitated as microparticles, when processed together, produce simultaneous precipitation again in form of microparticles: the complex behaviour of the quaternary system solvent – supercritical CO_2 – polymer – active compound can be different from the two ternary systems solvent – supercritical CO_2 – polymer or solvent – supercritical CO_2 – active compound [43].

In the case of SAS coprecipitation of complex mixtures like seed oils (passion fruit, grape) [97, 107] or green tea (extracts) [86] the prediction of the corresponding high pressure phase equilibria is not possible, but, successful coprecipitation could be still possible.

The most interesting new feature is the possibility that the selected polymer (mainly PVP) can correct the precipitation mechanism of the process compound; i.e., an active compound that, when alone, was unsuccessfully precipitated by SAS, can produce microparticles when coprecipitated with a proper polymer that can block the tendency of the active principle in producing uncontrolled crystals, by wrapping it inside the macromolecular structure [79, 83, 105, 113, 119-123, 125-127].

The mechanism proposed by some authors [109] of polymer nucleation followed by heterogeneous nucleation of the active principle is not only not probable; but, it is also not able to justify the formation of spherical composite amorphous microparticles.

3.1.2 Nanoparticles

Nerome et al. [71] proposed the formation of Lycopene/β-cyclodextrin inclusion complexes, precipitated from DMSO using SAS, obtaining nanoparticles at 100-140 bar and 40-50 °C. They carried out DSC analyses to examine the melting point of the processed powder in comparison with the raw materials and observed that the characteristic peaks of both the compounds disappeared in coprecipitated particles; therefore, they concluded that the formation of the inclusion complex was successful. However, other analyses, such as in vitro dissolution tests, were not performed to show the possible improvement of lycopene dissolution rate.

Garcia-Casas et al. [72] investigated the influence of the polymer/drug ratio in the coprecipitation of CAP/Quercetin from AC at 90 bar and 40 °C. The polymer/drug ratio was varied from 1/1 to 10/1 w/w, but in all cases, samples were formed by NP and crystals, suggesting the possible formation of a physical mixture of CAP and Quercetin. This hypothesis was confirmed by in vitro dissolution tests: SAS processed Quercetin showed a higher dissolution rate than CAP/Quercetin.

Montes et al. attempted the coprecipitation of Eudragit with Ibuprofene [76] and Naproxen [78]. In the first case, they observed that using AC as solvent and working at 120-200 bar and 40 °C, nanoparticles were produced; whereas, at 120 bar and 50 °C sub-microparticles were obtained. This result is unusual since in the SAS literature, it has been frequently observed that solutes precipitate from AC in form of NP. De Marco et al. [133], studying the behavior of solvents in contact with sc-CO_2 using elastic light scattering, found that this phenomenon occurs for AC because its transition region between two-phase and one-phase mixing (in which MP are produced) takes place in a very

narrow range of pressure. The results obtained by Montes et al., could be due to an enlargement of the miscibility gap between AC and CO_2 because of a partial solubility of one or both the compounds in the mixture solvent/antisolvent at the investigated conditions. Nevertheless, for both morphologies, drug release analyses carried out in simulated gastric fluid (SGF) and simulated intestinal fluid (SIF) showed that the drug bioavailability was not improved: the release rate of SAS processed particles was lower than the one of unprocessed ibuprofene. This evidence, along with DSC, XRD and FTIR analyses, suggests that coprecipitation probably failed and a micronized physical mixture was produced. For the system Eudragit/ Naproxen they obtained NP at 50 °C in the range 150-200 bar and SMP at 40 °C and 100 bar. Also in this case, drug release profiles did not show any improvement in the drug dissolution rate. Lam et al. [77] also used Eudragit as coating material for magnetite, to protect it from dissolution in the gastric fluid. They obtained nanoparticles from ethanol at 160 bar and 15-35 °C. Using X-ray Photoelectron Spectroscopy, the authors found encapsulation efficiencies in the range 36.5 - 70.1 % and employing a vibrating sample magnetometer they observed that the supermagnetic properties of Magnetite were preserved. Nevertheless, dissolution tests in SGF were not performed to verify if coprecipitation was successful or samples were formed by a nanometric physical mixture of Eudragit and Magnetite.

Djerafi et al. [74] investigated the roles of the kind of solvent and the polymer/drug ratio on SAS coprecipitation of Rifampicin and Ethyl cellulose. They observed that when EtAc was used at 100 bar, 35-60 °C and ratios 2/1-4/1, NP and crystals were obtained; it indicates that probably the two compounds precipitated separately. Conversely, when a mixture EtAc/DMSO 70/30 was employed, the same morphologies were observed in correspondence of a polymer/drug ratio of 1/1, whereas at 2/1 and 4/1 only NP were recovered. The authors reported drug release analyses showing that these last samples were more suitable for a sustained rifampicin release, but the curve related to the raw drug was not reported to support this statement. Park et al. [124] also studied the influence

of the solvent on the coprecipitation of PVP/Hydrochlorothiazide. They first carried out some experiments using DMSO at 86-190 bar and 30-40 °C: at all the conditions, NP were produced. This result is unusual since usually solutes precipitate from this solvent in form of MP since it shows a transition from subcritical to completely developed supercritical conditions in a wide range of pressure [139]. Moreover, both the compounds, when processed alone by SAS, precipitate in form of MP [124, 133]. When DMSO/AC was employed, NP were still obtained, but with a smaller mean size; this result is in agreement with the observations of De Marco et al. [133], who noted that the addition of AC to DMSO shrinks the phase transition and, therefore, the attainment of NP is favoured. Park et al. [124] affirmed that precipitation was successful; however, looking carefully at the TEM image reported in the paper, it is possible to observe that the dark shades, which indicate the presence of the drug, are not well uniformly distributed, suggesting the possible formation of a nanometric physical mixture. In vitro release tests were also reported; they showed that the drug dissolution rate for the SAS processed powder was 2 times faster than the unprocessed Hydrochlorothiazide; but, this result could be related to the higher surface area of the NP. Elizondo et al. [118] investigated the effect of the polymer/drug ratio in the coprecipitation of PVM-MA/Gentamicin-AOT and observed that increasing the ratio from 1/1 to 10/1 w/w, the particle morphology moved from NP to MP and that drug loading and entrapment efficiency decreased progressively. The authors carried out EDX analyses on a physical mixture of the two compounds and on SAS processed sample formed by nanoparticles; they observed that Sulphur, the characteristic element of Gentamicin-AOT, was located only in specific areas in the physical mixture; whereas, it was uniformly dispersed in the SAS processed powder. However, in vitro release tests were performed only for SAS samples formed by NP and they were not compared with the dissolution profile of the raw antibiotic, to confirm the occurrence of the coprecipitation; indeed, samples could be formed by a finely dispersed nanometric physical mixture.

Ha et al. proposed the addition of surfactants (Gelucire, Poloxamer and D-α-Tocopheryl polyethylene glycol 1000 succinate) on HPMC/Lercanidipine [81] and HPMC/Megestrol acetate [82] using EtOH/DCM as solvent and working at 150 bar and 40 °C. They observed that, when surfactants were employed, SMP with improved dissolution rate were obtained; whereas, in absence of surfactants, NP were produced, for which the drug dissolution rate was closer to that of the raw material.

Jin et al. [80] investigated the effect of the feed solution concentration on the formation of nanoparticles HPMCP/Insulin. They observed that working at low concentration, nanoparticles were obtained, but they stated that coprecipitation was unsuccessful since drug loading was lower than the initial one; increasing the overall concentration, drug loading increased and a successful coprecipitation was claimed. However, in vitro release tests in different medium were reported only for one SAS processed sample and a comparison with raw Insulin was not shown. Ha et al. [79] processed the systems HPC/Ezetimibe and PVP/Ezetimibe using EtOH as solvent. They observed that working in the range 120-180 bar and 40-50 °C for HPC/Ezetimibe and 150 bar, 40 °C for PVP/Ezetimibe, nanoparticles were produced; moreover, they observed that increasing the total concentration from 25 to 50-100 mg/mL SMP/MP were obtained. The authors carried out drug release tests comparing the dissolution profiles of raw Ezetimibe with the profiles of SAS produced NP; nanoparticles showed a significant increase in the drug dissolution rate, but the authors did not perform the analyses for the SMP/MP to investigate how the dissolution behavior changes with the different morphology. Chhouk et al. [70] proposed the coprecipitation of Curcumin using PVP as carrier and, working with AC/EtOH at 100-200 bar and 30-50 °C, they obtained NP and SMP.

Several paper in the literature showed the possibility to produce nanoparticles by SAS coprecipitation; however, as it is possible to deduce form the abovementioned results, many papers did not demonstrate with enough experimental evidences the success of coprecipitation. Moreover,

an explanation of the involved mechanisms is generally missing. The general mechanism of nanoparticles precipitation, as for single SAS compounds precipitation [52], requires homogeneous nucleation and growth from a gas phase. When two compounds are dissolved in the solution, each compound will tend to nucleate separately, producing separate nanoparticles. The formation of composite nanoparticles would require the occurrence of heterogeneous nucleation; i.e., nucleation of the active compound on which the polymer precipitates or polymer wrapping of active compound nanoclusters. The latter mechanism, however, should require very high quantities of polymer with respect to those of the active compound. It has been reported in literature [140] that when the supersaturation is high, as in the case of gas mixing, heterogeneous nucleation does not take place and the mechanism governing the precipitation is the primary homogeneous nucleation.The two previously described nucleation mechanisms are not frequent but cannot be excluded. The authors should carefully verify that separate precipitation produced a physical nanometric mixture.

3.1.3 Crystals and other morphologies (films)

Franceschi et al. [93] and Priamo et al. [94] studied the coprecipitation of PHBV and β-carotene from DCM at 80 bar and 40 °C. They observed that the pure polymer precipitated in form of SMP; whereas the pure API precipitated in form of crystals; then the two compounds were processed together and crystals were obtained. Experiments at different pressures were not performed to verify if a different morphology could be obtained. The authors performed experiments varying the polymer/drug ratio and observed that the encapsulation efficiency increased up to 55 % increasing the concentration of β-carotene. Dissolution tests were not carried out to prove the success of the coprecipitation. In these papers, the authors used carbon dioxide mass fraction lower than the usual ones; indeed, they used a carbon dioxide mass fraction in the range 0.4-0.9 [93, 94]. Wang et al. [106] attempted the coprecipitation of Hydrocortisone and PLGA using either AC or MeOH/DCM as

solvents at 89.6 bar and 33 °C, using a carbon dioxide molar fraction equal to 0.4. They obtained in all cases large crystals. Encapsulation efficiency determination and in vitro release tests proved that coprecipitation was unsuccessful and that the two materials precipitated individually. Cheng et al. [85] proposed the encapsulation of lycopene with lecithin and α-tocopherol using DMF as solvent and working at 80-120 bar and 35 °C. At all the investigated conditions, they obtained crystals with a recovery of lycopene lower than 29.2 %. These evidences suggest that not only coprecipitation was unsuccessful, but also that part of lycopene was extracted by the mixture solvent/antisolvent.In vitro release tests or other similar techniques were not reported to get information about the composition of the powder. Similar results were reported by Lang et al. [89] for the coprecipitation of PEG and Emodin from DCM/MeOH. They varied the pressure in the range 80-200 bar and the temperature in the range 35-50 °C, obtaining crystals that were not characterized to gain more data about the occurrence of the encapsulation. Majerik at al. [91] investigated the roles of the polymeric carrier and the liquid solvent on the coprecipitation of Oxeglitazer. When Poloxamer was used, experiments were carried out at 80 bar, 35 °C, using EtOH/CHF and DCM as solvents; in both the cases needle-like crystals were obtained. The same morphology was observed processing PEG from CHF at the same process conditions. Using PVP from DCM and CHF, instead, plate-like crystals were formed. Dissolution tests showed an improvement of the drug dissolution rate for the SAS processed powders compared to the raw material. Martín et al. [87] and He et al. [88] processed PEG/carotene from DCM by SAS at 35-50 °C and 80 and 160 bar, respectively. In both papers, the obtained powders were formed by PEG particles and carotene crystals, suggesting a failure in coprecipitation; dissolution tests were not reported for further investigation. Some authors [104, 115] produced films of PLGA/5-fluoracil and PLLA/Zidovudine, working in batch conditions.

The above reported experimental evidences suggest that crystals are obtained because at the employed process conditions, the operating point is often located in the biphasic region of the

system solvent/antisolvent and the liquid-like crystallization mechanism takes place. Sometimes, the partial solubility of one or both the compounds in CO_2 can induce a modification of the miscibility gap and, consequently, the operating point that should be located at supercritical conditions, falls in the vapor/liquid region. In other cases, the drug is characterized by a very fast crystallization kinetic that superimposes on precipitation. In this context, as mentioned before, an accurate selection of the carrier can avoid this phenomenon. Films formation could depend on the incomplete elimination of the liquid solvent that remains on the bottom of the precipitator or is released from the gas phase during the depressurization step. In all cases, the process fails.

4. CONCLUSIONS AND PERSPECTIVES

The production of micro/nanometric coprecipitates by supercritical antisolvent precipitation is a relevant process in view of the possible industrial applications. However, it revealed to be more complex as expected. It is not sufficient that both compounds involved (polymer and active principle) are singularly micronizable by SAS; their interactions with VLE at high pressure can modify their processability. In some cases, the proper polymer can make the active principle processable by SAS. Only the papers discussing micrometric coprecipitates are fully convincing about the successful operation and the formation mechanism of droplets drying proposed in this work explains their formation comprehensively.

Nano-coprecipitates are even more interesting, however, the experimental results are not always convincing. The underlying classical formation mechanisms confirms the difficulty of heterogeneous, simultaneous precipitation. The other morphologies generally produce uncontrolled growth of the solid matter. Indeed, the relevant SAS coprecipitation mechanism remains the competition of interfacial tension vanishing time and jet break-up time. However, it is well known that the SAS process requires as a pre-requisite that VLE of the system formed in the SAS precipitator allow solute precipitation: if a multiphase system is formed, other processes can

prevail, inducing, for example, crystals formation. Moreover, the presence of two or more solutes makes the corresponding VLE more complicated and, consequently, the possibility of successful coprecipitation is reduced. This consideration is the one that connects successful SAS precipitation and coprecipitation: SAS coprecipitation mechanisms are substantially the same as simple precipitation, as soon as, the proper VLE operate.

In conclusion, more work is still required in this field to obtain more general rules for successful SAS coprecipitation.

REFERENCES

[1] S. Brousseau, Z. Wang, S.K. Gupta, S.A. Meenach, Development of Aerosol Phospholipid Microparticles for the Treatment of Pulmonary Hypertension, AAPS PharmSciTech, (2017).
[2] L. Garcia-Contreras, D.J. Padilla-Carlin, J. Sung, J. VerBerkmoes, P. Muttil, K. Elbert, C. Peloquin, D. Edwards, A. Hickey, Pharmacokinetics of Ethionamide Delivered in Spray-Dried Microparticles to the Lungs of Guinea Pigs, Journal of Pharmaceutical Sciences, 106 (2017) 331-337.
[3] N.N. Pardeshi, W. Qi, K. Dahl, L. Caplan, J.F. Carpenter, Microparticles and Nanoparticles Delivered in Intravenous Saline and in an Intravenous Solution of a Therapeutic Antibody Product, Journal of Pharmaceutical Sciences, 106 (2017) 511-520.
[4] A. Ellis, J.C. Jacquier, Manufacture and characterisation of agarose microparticles, J. Food Eng., 90 (2009) 141-145.
[5] Y.-q. Kong, D. Li, L.-j. Wang, B. Adhikari, Preparation of gelatin microparticles using water-in-water (w/w) emulsification technique, J. Food Eng., 103 (2011) 9-13.
[6] V. Prosapio, E. Reverchon, I. De Marco, Antisolvent micronization of BSA using supercritical mixtures carbon dioxide+ organic solvent, J. Supercrit. Fluids, 94 (2014) 189-197.
[7] J. Zhang, X. Zhu, Y. Zhang, Preparation and Characterization of Titania Microspheres and Their Application in a Liquid Chromatography Stationary Phase, Journal of Crystallization Process and Technology, 6 (2016) 21.
[8] W. Zhao, K. Hu, C. Hu, X. Wang, A. Yu, S. Zhang, Silica gel microspheres decorated with covalent triazine-based frameworks as an improved stationary phase for high performance liquid chromatography, Journal of Chromatography A, 1487 (2017) 83-88.
[9] Z. Song, C. Duan, M. Shi, S. Li, Y. Guan, One-step preparation of ZrO2/SiO2 microspheres and modification with d-fructose 1, 6-bisphosphate as stationary phase for hydrophilic interaction chromatography, Journal of Chromatography A, (2017).
[10] G.L. Castiglioni, J. Cuellar, R. Rodrigo, J.A.V. Costa, R. Monte-Alegre, Application of Poly(styrene-co-divinylbenzene) Macroporous Microparticles as a Catalyst Support in the Enzymatic Synthesis of Biodiesel, Journal of Polymers and the Environment, 24 (2016) 264-273.
[11] J. Kim, S.H. Jin, K.-K. Kang, Y.-M. Chung, C.-S. Lee, Preparation of chemically uniform and monodisperse microparticles as highly efficient solid acid catalysts for aldol condensation, Chem. Eng. Sci., (2017).
[12] Y. Zhou, C. Li, J. Fu, C. Yu, X.-C. Hu, Nitrogen-doped graphene/tungsten oxide microspheres as an electro-catalyst support for formic acid electro-oxidation, RSC Advances, 6 (2016) 92852-92856.
[13] L. Hong, J. Guo, Y. Gao, W.-K. Yuan, Precipitation of Microparticulate Organic Pigment Powders by a Supercritical Antisolvent Process, Ind. Eng. Chem. Res., 39 (2000) 4882-4887.
[14] M. Maekawa, D. Honda, M. Enomura, Copper phthalocyanine pigment and method for producing copper phthalocyanine microparticles, in, Google Patents, 2016.
[15] C.W. Chang-Jian, E.C. Cho, S.C. Yen, B.C. Ho, K.C. Lee, J.H. Huang, Y.S. Hsiao, Facile preparation of WO3/PEDOT:PSS composite for inkjet printed electrochromic window and its performance for heat shielding, Dyes and Pigments, 148 (2018) 465-473.
[16] S.W. Oh, C.W. Kim, H.J. Cha, U. Pal, Y.S. Kang, Encapsulated-Dye All-Organic Charged Colored Ink Nanoparticles for Electrophoretic Image Display, Advanced Materials, 21 (2009) 4987-4991.
[17] M. Comet, B. Siegert, V. Pichot, P. Gibot, D. Spitzer, Preparation of explosive nanoparticles in a porous chromium(III) oxide matrix: a first attempt to control the reactivity of explosives, Nanotechnology, 19 (2008) 285716-285724.
[18] H. Langhals, Brightly shining nanoparticles: lipophilic perylene bisimides in aqueous phase, New Journal of Chemistry, 32 (2008) 21-23.
[19] J. George, S.N. Sabapathi, Cellulose nanocrystals: synthesis, functional properties, and applications, Nanotechnology, Science and Applications, 8 (2015) 45-54.
[20] A.J. Crosby, J.Y. Lee, Polymer Nanocomposites: The “Nano” Effect on Mechanical Properties, Polymer Reviews, 47 (2007) 217-229.
[21] I. Posadas, S. Monteagudo, V. Ceña, Nanoparticles for brain-specific drug and genetic material delivery, imaging and diagnosis, Nanomedicine, 11 (2016) 833-849.
[22] S.E.-S. Radwan, M.S. Sokar, D.A. Abdelmonsif, A.H. El-Kamel, Mucopenetrating nanoparticles for enhancement of oral bioavailability of furosemide: In vitro and in vivo evaluation/sub-acute toxicity study, Int. J. Pharm., 526 (2017) 366-379.
[23] A.A. McBride, D.N. Price, P. Muttil, Preparation and Characterization of Magnetic Nano-in-Microparticles for Pulmonary Delivery, Cancer Nanotechnology: Methods and Protocols, (2017) 99-108.

[24] E. Esposito, R. Roncarati, R. Cortesi, F. Cervellati, C. Nastruzzi, Production of Eudragit Microparticles by Spray-Drying Technique: Influence of Experimental Parameters on Morphological and Dimensional Characteristics, Pharmaceutical Development and Technology, 5 (2000) 267-278.
[25] S.A. Shoyele, S. Cawthorne, Particle engineering techniques for inhaled biopharmaceuticals, Adv. Drug Delivery Rev., 58 (2006) 1009-1029.
[26] H.J. Lee, J.H. Kang, H.G. Lee, D.W. Kim, Y.S. Rhee, J.Y. Kim, E.S. Park, C.W. Park, Preparation and physicochemical characterization of spray-dried and jet-milled microparticles containing bosentan hydrate for dry powder inhalation aerosols, Drug Design, Development and Therapy, 10 (2016) 4017-4030.
[27] X. Chang, J. Bao, G. Shan, Y. Bao, P. Pan, Crystallization-Driven Formation of Diversified Assemblies for Supramolecular Poly(lactic acid)s in Solution, Crystal Growth and Design, 17 (2017) 2498-2506.
[28] A.A. Thorat, S.V. Dalvi, Liquid antisolvent precipitation and stabilization of nanoparticles of poorly water soluble drugs in aqueous suspensions: Recent developments and future perspective, Chem. Eng. J., 181– 182 (2012) 1–34.
[29] Q. Zhang, Y. Han, W.-C. Wang, L. Zhang, J. Chang, Preparation of fluorescent polystyrene microspheres by gradual solvent evaporation method, European Polymer Journal, 45 (2009) 550-556.
[30] H. Salmani, I.M. Zorin, A.V. Akentiev, A.Y. Bilibin, Effect of preparation conditions on properties of polylactide and polystyrene and their composite microparticles made by emulsion solvent evaporation method, Polymer Science - Series A, 58 (2016) 744-753.
[31] L. Zhang, P. Liu, T. Wang, Preparation of superparamagnetic polyaniline hybrid hollow microspheres in oil/water emulsion with magnetic nanoparticles as cosurfactant, Chem. Eng. J., 171 (2011) 711-716.
[32] S. Omi, K.i. Katami, A. Yamamoto, M. Iso, Synthesis of polymeric microspheres employing SPG emulsification technique, J. Appl. Polym. Sci., 51 (1994) 1-11.
[33] T. Morita, Y. Horikiri, T. Suzuki, H. Yoshino, Preparation of gelatin microparticles by co-lyophilization with poly(ethylene glycol): characterization and application to entrapment into biodegradable microspheres, Int. J. Pharm., 219 (2001) 127-137.
[34] W. Wang, G. Liu, J. Wu, Y. Jiang, Co-precipitation of 10-hydroxycamptothecin and poly (l-lactic acid) by supercritical CO 2 anti-solvent process using dichloromethane/ethanol co-solvent, J. Supercrit. Fluids, 74 (2013) 137-144.
[35] A. Montes, R. Merino, D.M. De Los Santos, C. Pereyra, E.J. Martínez De La Ossa, Micronization of vanillin by rapid expansion of supercritical solutions process, J. CO2 Util., 21 (2017) 169-176.
[36] E. Reverchon, P. Pallado, Hydrodynamic modeling of the RESS process, J. Supercrit. Fluids, 9 (1996) 216-221.
[37] Á. Martín, H.M. Pham, A. Kilzer, S. Kareth, E. Weidner, Micronization of polyethylene glycol by PGSS (Particles from Gas Saturated Solutions)-drying of aqueous solutions, Chem. Eng. Process., 49 (2010) 1259-1266.
[38] H.T. Wu, S.C. Huang, C.P. Yang, L.J. Chien, Precipitation parameters and the cytotoxicity of chitosan hydrochloride microparticles production by supercritical assisted atomization, J. Supercrit. Fluids, 102 (2015) 123-132.
[39] E. Reverchon, A. Antonacci, Polymer microparticles production by supercritical assisted atomization, J. Supercrit. Fluids, 39 (2007) 444-452.
[40] J. Kluge, L. Joss, S. Viereck, M. Mazzotti, Emulsion crystallization of phenanthrene by supercritical fluid extraction of emulsions, Chem. Eng. Sci., 77 (2012) 249-258.
[41] G. Della Porta, E. Reverchon, Nanostructured microspheres produced by supercritical fluid extraction of emulsions, Biotechnology and Bioengineering, 100 (2008) 1020-1033.
[42] M. Rueda, L.M. Sanz-Moral, J.J. Segovia, Á. Martín, Enhancement of hydrogen release kinetics from ethane 1,2 diamineborane (EDAB) by micronization using Supercritical Antisolvent (SAS) precipitation, Chem. Eng. J., 306 (2016) 164-173.
[43] R. Campardelli, E. Reverchon, I. De Marco, Dependence of SAS particle morphologies on the ternary phase equilibria, J. Supercrit. Fluids, 130 (2017) 273-281.
[44] R.T. Bustami, H.-K. Chan, T. Sweeney, F. Dehghani, N.R. Foster, Generation of fine powders of recombinant human deoxyribonuclease using the aerosol solvent extraction system, Pharm. Res., 20 (2003) 2028-2035.
[45] D.L. Boschetto, E.M. Aranha, A.A.U. de Souza, S.M.A.G.U. Souza, S.R.S. Ferreira, W.L. Priamo, J.V. Oliveira, Encapsulation of bixin in PHBV using SEDS technique and in vitro release evaluation, Industrial Crops and Products, 60 (2014) 22-29.
[46] P. Chattopadhyay, R.B. Gupta, Production of Antibiotic Nanoparticles Using Supercritical CO2 as Antisolvent with Enhanced Mass Transfer, Ind. Eng. Chem. Res., 40 (2001) 3530-3539.
[47] I. De Marco, V. Prosapio, F. Cice, E. Reverchon, Use of solvent mixtures in supercritical antisolvent process to modify precipitates morphology: Cellulose acetate microparticles, J. Supercrit. Fluids, 83 (2013) 153-160.
[48] N. Esfandiari, Production of micro and nano particles of pharmaceutical by supercritical carbon dioxide, J. Supercrit. Fluids, 100 (2015) 129-141.
[49] N.R. Foster, F. Dehghani, K.M. Charoenchaitrakoo, B. Warwick, Application of dense gas techniques for the production of fine particles, AAPS pharmSci [electronic resource], 5 (2003).

[50] M. Rossmann, A. Braeuer, A. Leipertz, E. Schluecker, Manipulating the size, the morphology and the polymorphism of acetaminophen using supercritical antisolvent (SAS) precipitation, J. Supercrit. Fluids, 82 (2013) 230-237.
[51] A. Tenorio, M.D. Gordillo, C. Pereyra, E.J. Martinez de la Ossa, Controlled submicro particle formation of ampicillin by supercritical antisolvent precipitation, J. Supercrit. Fluids, 40 (2007) 308-316.
[52] E. Reverchon, I. De Marco, Mechanisms controlling supercritical antisolvent precipitate morphology, Chem. Eng. J., 169 (2011) 358-370.
[53] A. Montes, L. Wehner, C. Pereyra, E.J. Martínez de la Ossa, Mangiferin nanoparticles precipitation by supercritical antisolvent process, J. Supercrit. Fluids, 112 (2016) 44-50.
[54] T.J. Yoon, W.-S. Son, H.J. Park, B. Seo, T. Kim, Y.-W. Lee, Tetracycline nanoparticles precipitation using supercritical and liquid CO2 as antisolvents, J. Supercrit. Fluids, 107 (2016) 51-60.
[55] I. Garay, A. Pocheville, L. Madariaga, Polymeric microparticles prepared by supercritical antisolvent precipitation, Powder Technol., 197 (2010) 211-217.
[56] S.-C. Chang, M.-J. Lee, H.-M. Lin, Role of phase behavior in micronization of lysozyme via a supercritical anti-solvent process, Chem. Eng. J., 139 (2008) 416-425.
[57] E. Reverchon, I. De Marco, R. Adami, G. Caputo, Expanded micro-particles by supercritical antisolvent precipitation: interpretation of results, J. Supercrit. Fluids, 44 (2008) 98-108.
[58] I.A. Cuadra, A. Cabañas, J.A.R. Cheda, F.J. Martínez-Casado, C. Pando, Pharmaceutical co-crystals of the anti-inflammatory drug diflunisal and nicotinamide obtained using supercritical CO2 as an antisolvent, J. CO2 Util., 13 (2016) 29-37.
[59] H.J. Park, M.-S. Kim, S. Lee, J.-S. Kim, J.-S. Woo, J.-S. Park, S.-J. Hwang, Recrystallization of fluconazole using the supercritical antisolvent (SAS) process, Int. J. Pharm., 328 (2007) 152-160.
[60] S. Takenouchi, G.C. Kennedy, The binary system H_2O-CO_2 at high temperatures and pressures, American Journal of Science, 262 (1964) 1055-1074.
[61] I. De Marco, E. Reverchon, Supercritical carbon dioxide+ ethanol mixtures for the antisolvent micronization of hydrosoluble materials, Chem. Eng. J., 187 (2012) 401-409.
[62] V. Prosapio, E. Reverchon, I. De Marco, Polymers' ultrafine particles for drug delivery systems precipitated by supercritical carbon dioxide + organic solvent mixtures, Powder Technol., 292 (2016) 140-148.
[63] S.M.H. Hosseini, Z. Emam-Djomeh, P. Sabatino, P. Van der Meeren, Nanocomplexes arising from protein-polysaccharide electrostatic interaction as a promising carrier for nutraceutical compounds, Food Hydrocolloids, 50 (2015) 16-26.
[64] A. Montes, M.D. Gordillo, C. Pereyra, E.J. Martínez de la Ossa, Co-precipitation of amoxicillin and ethyl cellulose microparticles by supercritical antisolvent process, J. Supercrit. Fluids, 60 (2011) 75-80.
[65] P.K. Okuro, F. Eustáquio de Matos, C.S. Favaro-Trindade, Technological challenges for spray chilling encapsulation of functional food ingredients, Food Technol. Biotech., 51 (2013) 171-182.
[66] L.Y. Lee, C.H. Wang, K.A. Smith, Supercritical antisolvent production of biodegradable micro- and nanoparticles for controlled delivery of paclitaxel, J. Control. Release, 125 (2008) 96-106.
[67] Y. Wang, R. Pfeffer, R. Dave, R. Enick, Polymer encapsulation of fine particles by a supercritical antisolvent process, AIChE Journal, 51 (2005) 440-455.
[68] A. Martín, M.J. Cocero, Micronization processes with supercritical fluids: Fundamentals and mechanisms, Adv. Drug Delivery Rev., 60 (2008) 339-350.
[69] D.J. Jarmer, C.S. Lengsfeld, T.W. Randolph, Manipulation of particle size distribution of poly(l-lactic acid) nanoparticles with a jet-swirl nozzle during precipitation with a compressed antisolvent, J. Supercrit. Fluids, 27 (2003) 317-336.
[70] K. Chhouk, Wahyudiono, H. Kanda, S.-I. Kawasaki, M. Goto, Micronization of curcumin with biodegradable polymer by supercritical anti-solvent using micro swirl mixer, Frontiers of Chemical Science and Engineering, (2017).
[71] H. Nerome, S. Machmudah, Wahyudiono, R. Fukuzato, T. Higashiura, Y.S. Youn, Y.W. Lee, M. Goto, Nanoparticle formation of lycopene/β-cyclodextrin inclusion complex using supercritical antisolvent precipitation, J. Supercrit. Fluids, 83 (2013) 97-103.
[72] I. García-Casas, A. Montes, C. Pereyra, E.J. Martínez de la Ossa, Generation of quercetin/cellulose acetate phthalate systems for delivery by supercritical antisolvent process, Eur. J. Pharm. Sci., 100 (2017) 79-86.
[73] A. Montes, M.D. Gordillo, C. Pereyra, E.J. Martínez de la Ossa, Polymer and ampicillin co-precipitation by supercritical antisolvent process, J. Supercrit. Fluids, 63 (2012) 92-98.
[74] R. Djerafi, A. Swanepoel, C. Crampon, L. Kalombo, P. Labuschagne, E. Badens, Y. Masmoudi, Supercritical antisolvent co-precipitation of rifampicin and ethyl cellulose, Eur. J. Pharm. Sci., 102 (2017) 161-171.
[75] A. Montes, L. Wehner, C. Pereyra, E.J. Martínez de la Ossa, Generation of microparticles of ellagic acid by supercritical antisolvent process, J. Supercrit. Fluids, 116 (2016) 101-110.

[76] A. Montes, M.D. Gordillo, C. Pereyra, D.M. De los Santos, E.J. Martínez de la Ossa, Ibuprofen–polymer precipitation using supercritical CO2 at low temperature, J. Supercrit. Fluids, 94 (2014) 91-101.
[77] U.T. Lam, R. Yoganathan, A.G. Carr, R. Mammucari, N.R. Foster, Encapsulation of Superparamagnetic Iron Oxide Nanoparticles by the Supercritical Antisolvent Process, Australian Journal of Chemistry, 65 (2012) 40-44.
[78] A. Montes, N. Kin, M.D. Gordillo, C. Pereyra, E.J. Martínez de la Ossa, Polymer–naproxen precipitation by supercritical antisolvent (SAS) process, J. Supercrit. Fluids, 89 (2014) 58-67.
[79] E.-S. Ha, J.-S. Kim, I.-h. Baek, S.-J. Hwang, M.-S. Kim, Enhancement of dissolution and bioavailability of ezetimibe by amorphous solid dispersion nanoparticles fabricated using supercritical antisolvent process, Journal of Pharmaceutical Investigation, 45 (2015) 641-649.
[80] H.Y. Jin, F. Xia, Y.P. Zhao, Preparation of hydroxypropyl methyl cellulose phthalate nanoparticles with mixed solvent using supercritical antisolvent process and its application in co-precipitation of insulin, Adv. Pow. Tech., 23 (2012) 157-163.
[81] E.-S. Ha, G.-H. Choo, I.-h. Baek, J.-S. Kim, W. Cho, Y.S. Jung, S.-E. Jin, S.-J. Hwang, M.-S. Kim, Dissolution and bioavailability of lercanidipine–hydroxypropylmethyl cellulose nanoparticles with surfactant, International Journal of Biological Macromolecules, 72 (2015) 218-222.
[82] E.S. Ha, J.S. Kim, I.H. Baek, J.W. Yoo, Y. Jung, H.R. Moon, M.S. Kim, Development of megestrol acetate solid dispersion nanoparticles for enhanced oral delivery by using a supercritical antisolvent process, Drug Design, Development and Therapy, 9 (2015) 4269-4277.
[83] J. Park, W. Cho, K.-H. Cha, J. Ahn, K. Han, S.-J. Hwang, Solubilization of the poorly water soluble drug, telmisartan, using supercritical anti-solvent (SAS) process, Int. J. Pharm., 441 (2013) 50-55.
[84] C.A. Ober, L. Kalombo, H. Swai, R.B. Gupta, Preparation of rifampicin/lactose microparticle composites by a supercritical antisolvent-drug excipient mixing technique for inhalation delivery, Powder Technol., 236 (2013) 132-138.
[85] Y.-S. Cheng, P.-M. Lu, C.-Y. Huang, J.-J. Wu, Encapsulation of lycopene with lecithin and α-tocopherol by supercritical antisolvent process for stability enhancement, J. Supercrit. Fluids, 130 (2017) 246-252.
[86] M.V. Sosa, S. Rodríguez-Rojo, F. Mattea, M. Cismondi, M.J. Cocero, Green tea encapsulation by means of high pressure antisolvent coprecipitation, J. Supercrit. Fluids, 56 (2011) 304-311.
[87] A. Martín, F. Mattea, L. Gutiérrez, F. Miguel, M.J. Cocero, Co-precipitation of carotenoids and bio-polymers with the supercritical anti-solvent process, J. Supercrit. Fluids, 41 (2007) 138-147.
[88] W. He, Q. Suo, H. Hong, A. Shan, C. Li, Y. Huang, Y. Li, M. Zhu, Production of natural carotene-dispersed polymer microparticles by SEDS-PA co-precipitation, Journal of Materials Science, 42 (2007) 3495-3501.
[89] Z.M. Lang, H.L. Hong, L.M. Han, N. Zhu, Q.L. Suo, Preparation of emodin-polyethylene glycol composite microparticles using a supercritical antisolvent process, Chemical Engineering and Technology, 35 (2012) 362-368.
[90] A.M. Barrett, F. Dehghani, N.R. Foster, Increasing the Dissolution Rate of Itraconazole Processed by Gas Antisolvent Techniques using Polyethylene Glycol as a Carrier, Pharm. Res., 25 (2007) 1274-1289.
[91] V. Majerik, G. Charbit, E. Badens, G. Horváth, L. Szokonya, N. Bosc, E. Teillaud, Bioavailability enhancement of an active substance by supercritical antisolvent precipitation, J. Supercrit. Fluids, 40 (2007) 101-110.
[92] I.-I. Jung, S. Haam, G. Lim, J.-H. Ryu, Preparation of peptide-loaded polymer microparticles using supercritical carbon dioxide, Biotechnology and Bioprocess Engineering, 17 (2012) 185-194.
[93] E. Franceschi, A.M. De Cesaro, M. Feiten, S.R.S. Ferreira, C. Dariva, M.H. Kunita, A.F. Rubira, E.C. Muniz, M.L. Corazza, J.V. Oliveira, Precipitation of β-carotene and PHBV and co-precipitation from SEDS technique using supercritical CO2, J. Supercrit. Fluids, 47 (2008) 259-269.
[94] W.L. Priamo, A.M. De Cezaro, S.R.S. Ferreira, J.V. Oliveira, Precipitation and encapsulation of β-carotene in PHBV using carbon dioxide as anti-solvent, J. Supercrit. Fluids, 54 (2010) 103-109.
[95] E. Franceschi, A. De Cezaro, S.R.S. Ferreira, M.H. Kunita, E.C. Muniz, A.F. Rubira, J.V. Oliveira, Co-precipitation of beta-carotene and bio-polymer using supercritical carbon dioxide as antisolvent, Open Chem. Eng. J., 4 (2010) 11-20.
[96] F.R.S. Machado, T.C. Trevisol, D.L. Boschetto, J.F.M. Burkert, S.R.S. Ferreira, J.V. Oliveira, C.A.V. Burkert, Technological process for cell disruption, extraction and encapsulation of astaxanthin from Haematococcus pluvialis, Journal of Biotechnology, 218 (2016) 108-114.
[97] D.L. Boschetto, I. Dalmolin, A.M. de Cesaro, A.A. Rigo, S.R.S. Ferreira, M.A.A. Meireles, E.A.C. Batista, J. Vladimir Oliveira, Phase behavior and process parameters effect on grape seed extract encapsulation by SEDS technique, Industrial Crops and Products, 50 (2013) 352-360.
[98] A. Argemí, A. Vega, P. Subra-Paternault, J. Saurina, Characterization of azacytidine/poly(l-lactic) acid particles prepared by supercritical antisolvent precipitation, Journal of Pharmaceutical and Biomedical Analysis, 50 (2009) 847-852.
[99] T.M. Martin, N. Bandi, R. Shulz, C.B. Roberts, U.B. Kompella, Preparation of budesonide and budesonide-PLA microparticles using supercritical fluid precipitation technology, AAPS PharmSciTech, 3 (2002) 16-26.

[100] R. Guha, M. Vinjamur, M. Mukhopadhyay, Demonstration of mechanisms for coprecipitation and encapsulation by supercritical antisolvent process, Ind. Eng. Chem. Res., 50 (2011) 1079-1088.
[101] N. Elvassore, A. Bertucco, P. Caliceti, Production of protein-loaded polymeric microcapsules by compressed CO2 in a mixed solvent, Ind. Eng. Chem. Res., 40 (2001) 795-800.
[102] F. Miguel, A. Martín, F. Mattea, M.J. Cocero, Precipitation of lutein and co-precipitation of lutein and poly-lactic acid with the supercritical anti-solvent process, Chem. Eng. Process., 47 (2008) 1594-1602.
[103] P.S.C. Sacchetin, R.F. Setti, P.d.T.V.e. Rosa, Â.M. Moraes, Properties of PLA/PCL particles as vehicles for oral delivery of the androgen hormone 17α-methyltestosterone, Materials Science and Engineering: C, 58 (2016) 870-881.
[104] P. Kalantarian, I. Haririan, A.R. Najafabadi, M.A. Shokrgozar, A. Vatanara, Entrapment of 5-fluorouracil into PLGA matrices using supercritical antisolvent processes, Journal of Pharmacy and Pharmacology, 63 (2011) 500-506.
[105] S. Lee, M.S. Kim, J.S. Kim, H.J. Park, J.S. Woo, B.C. Lee, S.J. Hwang, Controlled delivery of a hydrophilic drug from a biodegradable microsphere system by supercritical anti-solvent precipitation technique, Journal of Microencapsulation, 23 (2006) 741-749.
[106] Y. Wang, Y. Wang, J. Yang, R. Pfeffer, R. Dave, B. Michniak, The application of a supercritical antisolvent process for sustained drug delivery, Powder Technol., 164 (2006) 94-102.
[107] D.A. Oliveira, N. Mezzomo, C. Gomes, S.R.S. Ferreira, Encapsulation of passion fruit seed oil by means of supercritical antisolvent process, J. Supercrit. Fluids, 129 (2017) 96-105.
[108] A.-Z. Chen, X.-M. Pu, Y.-Q. Kang, L. Liao, Y.-D. Yao, G.-F. Yin, Preparation of 5-Fluorouracil-Poly(L-lactide) Microparticles Using Solution-Enhanced Dispersion by Supercritical CO2, Macromolecular Rapid Communications, 27 (2006) 1254-1259.
[109] C.G. Kalogiannis, C.M. Michailof, C.G. Panayiotou, Microencapsulation of amoxicillin in poly (l-lactic acid) by supercritical antisolvent precipitation, Ind. Eng. Chem. Res., 45 (2006) 8738-8743.
[110] S. Taki, E. Badens, G. Charbit, Controlled release system formed by supercritical anti-solvent coprecipitation of a herbicide and a biodegradable polymer, J. Supercrit. Fluids, 21 (2001) 61-70.
[111] W. Li, G. Liu, L. Li, J. Wu, Y. LÜ, Y. Jiang, Effect of Process Parameters on Co-precipitation of Paclitaxel and Poly(L-lactic Acid) by Supercritical Antisolvent Process, Chinese Journal of Chemical Engineering, 20 (2012) 803-813.
[112] L. Wenfeng, L. Guijin, L. Lixian, W. Juan, L. Yangxiao, Y. JIANG, Effect of process parameters on co-precipitation of paclitaxel and poly (l-lactic acid) by supercritical antisolvent process, Chinese Journal of Chemical Engineering, 20 (2012) 803-813.
[113] V. Patomchaiviwat, O. Paeratakul, P. Kulvanich, Formation of inhalable rifampicin–poly (L-lactide) microparticles by supercritical anti-solvent process, AAPS PharmSciTech, 9 (2008) 1119-1129.
[114] D. Alias, R. Yunus, G.H. Chong, C.A. Che Abdullah, Single step encapsulation process of tamoxifen in biodegradable polymer using supercritical anti-solvent (SAS) process, Powder Technol., 309 (2017) 89-94.
[115] V.M.H. Yoshida, V.M. Balcão, M.M.D.C. Vila, J.M. Oliveira Júnior, N. Aranha, M.V. Chaud, M.P.D. Gremião, Zidovudine-Poly(l-Lactic Acid) Solid Dispersions with Improved Intestinal Permeability Prepared by Supercritical Antisolvent Process, Journal of Pharmaceutical Sciences, 104 (2015) 1691-1700.
[116] N. Mezzomo, E.d. Paz, M. Maraschin, Á. Martín, M.J. Cocero, S.R.S. Ferreira, Supercritical anti-solvent precipitation of carotenoid fraction from pink shrimp residue: Effect of operational conditions on encapsulation efficiency, J. Supercrit. Fluids, 66 (2012) 342-349.
[117] M. Fraile, R. Buratto, B. Gómez, Á. Martín, M.J. Cocero, Enhanced Delivery of Quercetin by Encapsulation in Poloxamers by Supercritical Antisolvent Process, Ind. Eng. Chem. Res., 53 (2014) 4318-4327.
[118] E. Elizondo, S. Sala, E. Imbuluzqueta, D. González, M.J. Blanco-Prieto, C. Gamazo, N. Ventosa, J. Veciana, High loading of gentamicin in bioadhesive PVM/MA nanostructured microparticles using compressed carbon-dioxide, Pharm. Res., 28 (2011) 309-321.
[119] V. Prosapio, E. Reverchon, I. De Marco, Incorporation of liposoluble vitamins within PVP microparticles using supercritical antisolvent precipitation, J. CO2 Util., 19 (2017) 230-237.
[120] V. Prosapio, E. Reverchon, I. De Marco, Coprecipitation of Polyvinylpyrrolidone/β-Carotene by Supercritical Antisolvent Processing, Ind. Eng. Chem. Res., 54 (2015) 11568-11575.
[121] V. Prosapio, I. De Marco, E. Reverchon, PVP/corticosteroid microspheres produced by supercritical antisolvent coprecipitation, Chem. Eng. J., 292 (2016) 264-275.
[122] F. Zahran, A. Cabañas, J.A.R. Cheda, J.A.R. Renuncio, C. Pando, Dissolution rate enhancement of the anti-inflammatory drug diflunisal by coprecipitation with a biocompatible polymer using carbon dioxide as a supercritical fluid antisolvent, J. Supercrit. Fluids, 88 (2014) 56-65.
[123] V. Prosapio, I. De Marco, M. Scognamiglio, E. Reverchon, Folic acid–PVP nanostructured composite microparticles by supercritical antisolvent precipitation, Chem. Eng. J., 277 (2015) 286-294.
[124] H.J. Park, T.J. Yoon, D.E. Kwon, K. Yu, Y.-W. Lee, Coprecipitation of hydrochlorothiazide/PVP for the dissolution rate improvement by precipitation with compressed fluid antisolvent process, J. Supercrit. Fluids, 126 (2017) 37-46.

[125] V. Prosapio, E. Reverchon, I. De Marco, Formation of PVP/nimesulide microspheres by supercritical antisolvent coprecipitation, J. Supercrit. Fluids, 118 (2016) 19-26.
[126] K. Wu, J. Li, W. Wang, D.A. Winstead, Formation and characterization of solid dispersions of piroxicam and polyvinylpyrrolidone using spray drying and precipitation with compressed antisolvent, Journal of Pharmaceutical Sciences, 98 (2009) 2422-2431.
[127] D. Hu, C. Lin, L. Liu, S. Li, Y. Zhao, Preparation, characterization, and in vitro release investigation of lutein/zein nanoparticles via solution enhanced dispersion by supercritical fluids, J. Food Eng., 109 (2012) 545-552.
[128] C.S. Lengsfeld, J.P. Delplanque, V.H. Barocas, T.W. Randolph, Mechanism Governing Microparticle Morphology during Precipitation by a Compressed Antisolvent: Atomization vs Nucleation and Growth, The Journal of Physical Chemistry B, 104 (2000) 2725-2735.
[129] E. Reverchon, E. Torino, S. Dowy, A. Braeuer, A. Leipertz, Interactions of phase equilibria, jet fluid dynamics and mass transfer during supercritical antisolvent micronization, Chem. Eng. J., 156 (2010) 446-458.
[130] F. Chávez, P.G. Debenedetti, J. Luo, R.N. Dave, R. Pfeffer, Estimation of the characteristic time scales in the supercritical antisolvent process, Ind. Eng. Chem. Res., 42 (2003) 3156-3162.
[131] S.S. Dukhin, C. Zhu, R. Dave, R. Pfeffer, J.J. Luo, F. Chávez, Y. Shen, Dynamic interfacial tension near critical point of a solvent–antisolvent mixture and laminar jet stabilization, Colloids and Surfaces A: Physicochemical and Engineering Aspects, 229 (2003) 181-199.
[132] M. Sarkari, I. Darrat, B.L. Knutson, Generation of microparticles using CO2 and CO2-philic antisolvents, AIChE Journal, 46 (2000) 1850-1859.
[133] I. De Marco, M. Rossmann, V. Prosapio, E. Reverchon, A. Braeuer, Control of particle size, at micrometric and nanometric range, using supercritical antisolvent precipitation from solvent mixtures: Application to PVP, Chemical Engineering Journal, 273 (2015) 344-352.
[134] T. Petit-Gas, O. Boutin, I. Raspo, E. Badens, Role of hydrodynamics in supercritical antisolvent processes, J. Supercrit. Fluids, 51 (2009) 248-255.
[135] V. Patomchaiviwat, O. Paeratakul, P. Kulvanich, Formation of Inhalable Rifampicin–Poly(l-lactide) Microparticles by Supercritical Anti-solvent Process, AAPS PharmSciTech, 9 (2008) 1119-1129.
[136] A. Montes, L. Wehner, C. Pereyra, E.J. Martínez de la Ossa, Generation of microparticles of ellagic acid by supercritical antisolvent process, The Journal of Supercritical Fluids, 116 (2016) 101-110.
[137] W. Wang, G. Liu, J. Wu, Y. Jiang, Co-precipitation of 10-hydroxycamptothecin and poly (l-lactic acid) by supercritical CO2 anti-solvent process using dichloromethane/ethanol co-solvent, The Journal of Supercritical Fluids, 74 (2013) 137-144.
[138] C.G. Kalogiannis, C.M. Michailof, C.G. Panayiotou, Microencapsulation of Amoxicillin in Poly(l-lactic acid) by Supercritical Antisolvent Precipitation, Industrial & Engineering Chemistry Research, 45 (2006) 8738-8743.
[139] I. De Marco, O. Knauer, F. Cice, A. Braeuer, E. Reverchon, Interactions of phase equilibria, jet fluid dynamics and mass transfer during supercritical antisolvent micronization: The influence of solvents, Chemical Engineering Journal, 203 (2012) 71-80.
[140] P. York, U.B. Kompella, B.Y. Shekunov, Supercritical fluid technology for drug product development, CRC Press, 2004.